**Figure S1. Timeline of revascularization in OIR and depiction of laser-capture microdissection**

(**A**) Representative photo-micrographs of *Griffonia simplicifolia* lectin-stained retinal flatmounts illustrate the progression of vascular growth following the initial vaso-obliteration in response to oxygen exposure from P7-12. At P12, immediately after exposure to hyperoxia, retinas present maximal vascular loss. As the retina attempts to revascularize, there is an initial delay in regrowth followed by misdirected pre-retinal vascular tuft formation that peaks at P17. Subsequently at P19-21, vessels enter the avascular retina, as the pre-retinal neovascularization regresses. By P23, the vaso-obliterated zone is fully revascularized. (**B**) Representative retinal cross-section of lectin-stained normal vessels before laser-capture, compared to (pre-retinal) vascular tufts. Dotted lines represent the laser dissection.

**Figure S2. VEGF is upregulated in the central avascular region of the OIR retina**

Micro-dissection of avascular (A) and vascularized (V) areas of retinas from mice (P14) subjected to OIR, reveals a ~3-fold induction in VEGF protein (by Western blotting) specifically in the avascular center during pathological neovascularization (n=4). There is no significant difference in VEGF expression between peripheral (P) and central (C) normoxic retina at P14. Values are shown relative to peripheral and vascularized retinas ± s.e.m. *p=0.019 compared to corresponding vascularized area (V).

**Figure S3. Expression of IL-1R1 in RGC-5 and astrocytes.** (**A**) Protein expression of IL-1R1 in unstimulated rat RGC-5 (by Western blot); human Tf-1 cells were used as positive control (n=3). (**B**) Confocal immunohistochemical imaging of retinal cross-sections from P14 mice subjected to OIR reveals expression of IL-1R in astrocytes (GFAP positive); note merged images. n=3. Scale bar: 25 μm.

**Figure S4**. **Intravitreal injection of lentivirus efficiently infects RGCs.** (**A**) LV vectors containing a GFP transgene under a CMV promoter (Lv.GFP) were injected intravitreally into mouse pups at P2 and infected ~70% of RGCs as detected by co-localization with the RGC-specific marker Thy1.1. at P14 (n=3). (**B**) Intravitreal injections of Lv.shSema3A at P2 resulted in a ~38% reduction at P8 (n=3, *p=0.043) and ~54% reduction at P14 (n=3, *p=0.034) of Sema3A protein, relative to values for corresponding Lv.shGFP. (**C, D**) Specificity of shSema3A was confirmed as neither VEGF nor other related Semaphorins such as Sema3D, Sema3E or Sema3F were downregulated. n=3; ***p<0.005 compared to corresponding Lv.shGFP. Scale bar (**A**) 50 μm.

**Figure S5. Lv.shSema3A protects against vaso-obliteration and neovascularization** (**A**) Lectin-stained retinal flatmounts reveal that Lv.shSema3A treated retinas present significantly less vasoobliteration (67% relative to controls). n=13-15, **p=0.01 compared to control. (**B**) Neovascular areas shown in Figure 3B were quantified using Swift NV[1]; representative quantification masks are presented.

**Figure S6.** ***In vitro*** **assessment of RGC–derived Sema3A.** (**A**) Lentivirus efficiently infects cultured RGCs and shSema3A reduces Sema3A expression by ~50%. n=3; ***p<0.01 compared to control. (**B**) Time lapse images (0 to 45 min) of EC contraction upon stimulation with rSema3A (1 μg/ml) or vehicle (control). (**C**) Pull-down of activated RhoA-GTP reveals that this permissive player in cytoskeletal growth and remodelling becomes activated when RGC-derived Sema3A is knocked down in CM.

REFERENCES

1. Stahl A, Connor KM, Sapieha P, Willett KL, Krah NM, Dennison RJ, Chen J, Guerin KI, Smith LE. Computer-aided quantification of retinal neovascularization. *Angiogenesis.* 2009;12(3):297-301.

Figure S1

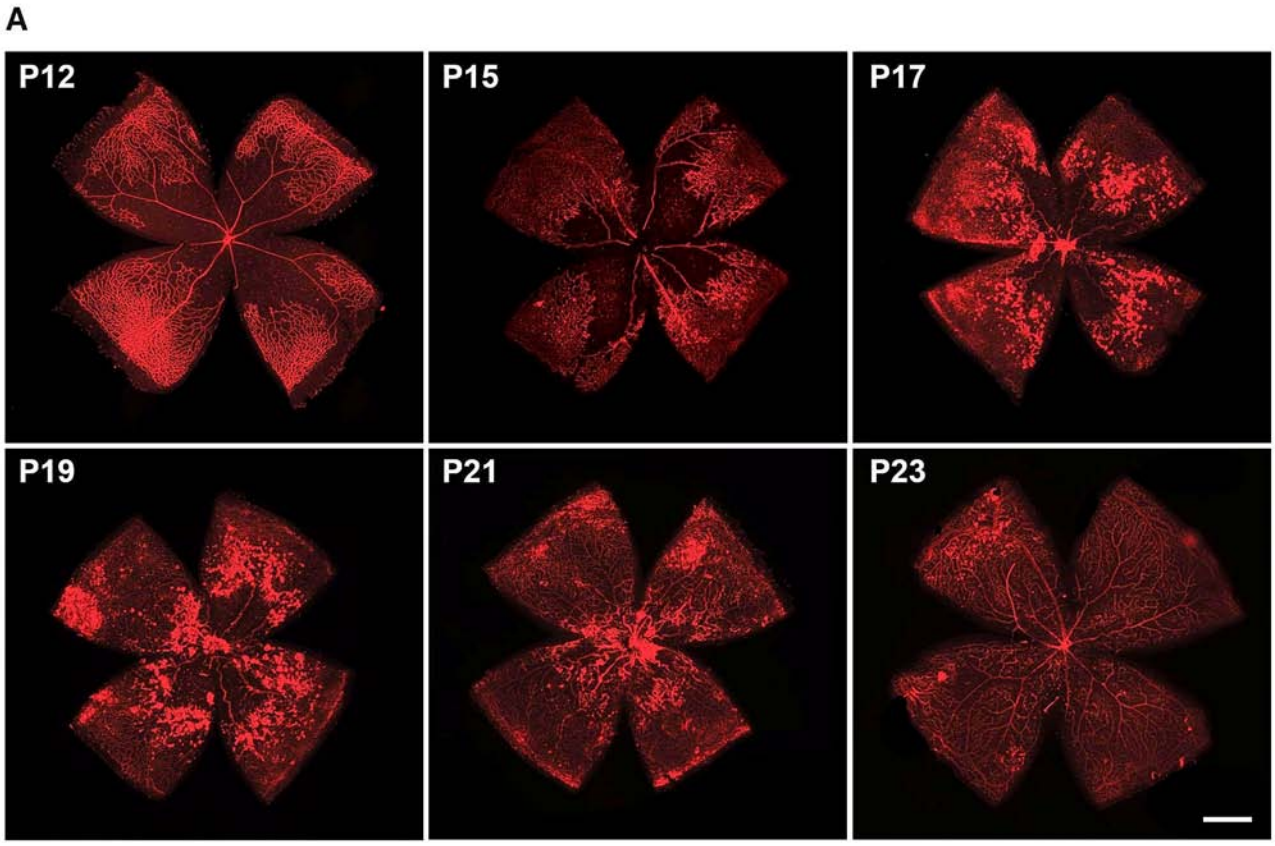
A
P12
P15
P17
P19
P21
P23

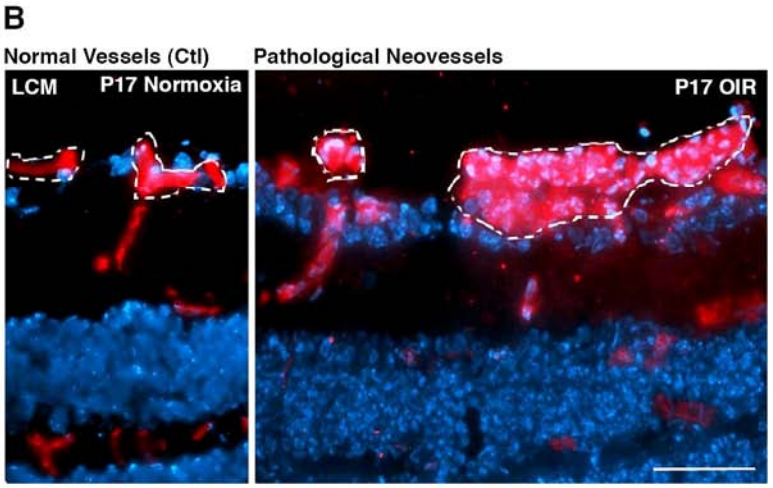
B
Normal Vessels (Ctl)
Pathological Neovessels
LCM
P17 Normoxia
P17 OIR

## Figure S2

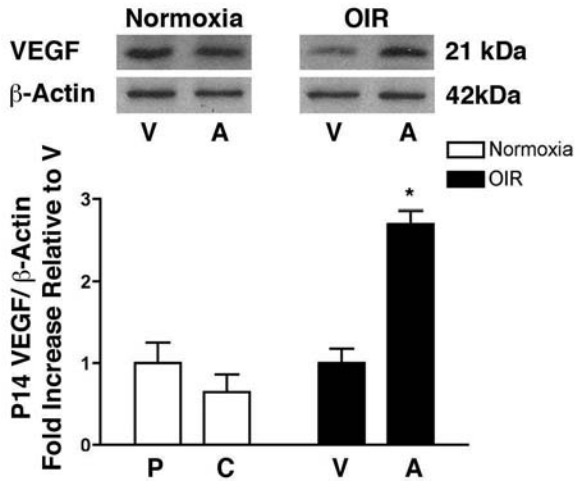
Normoxia
OIR
VEGF
β-Actin
21 kDa
42kDa
V
A
V
A
Normoxia
OIR
P14 VEGF/ β-Actin
Fold Increase Relative to V
3
2
1
0
*
P
C
V
A

Figure S3

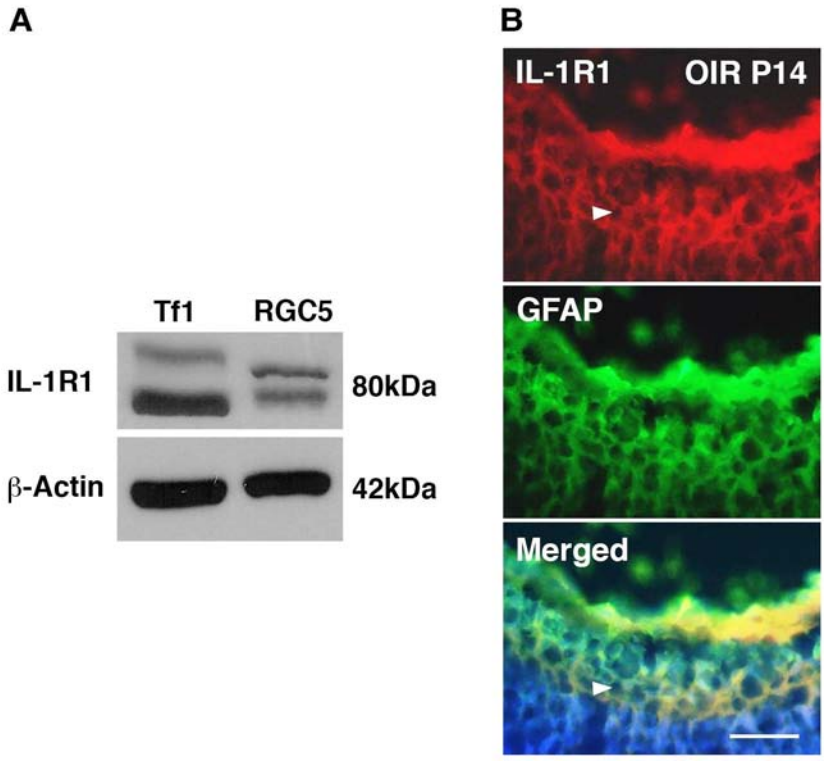
A
Tf1
RGC5
IL-1R1
80kDa
β-Actin
42kDa
B
IL-1R1
OIR P14
GFAP
Merged

Figure S4

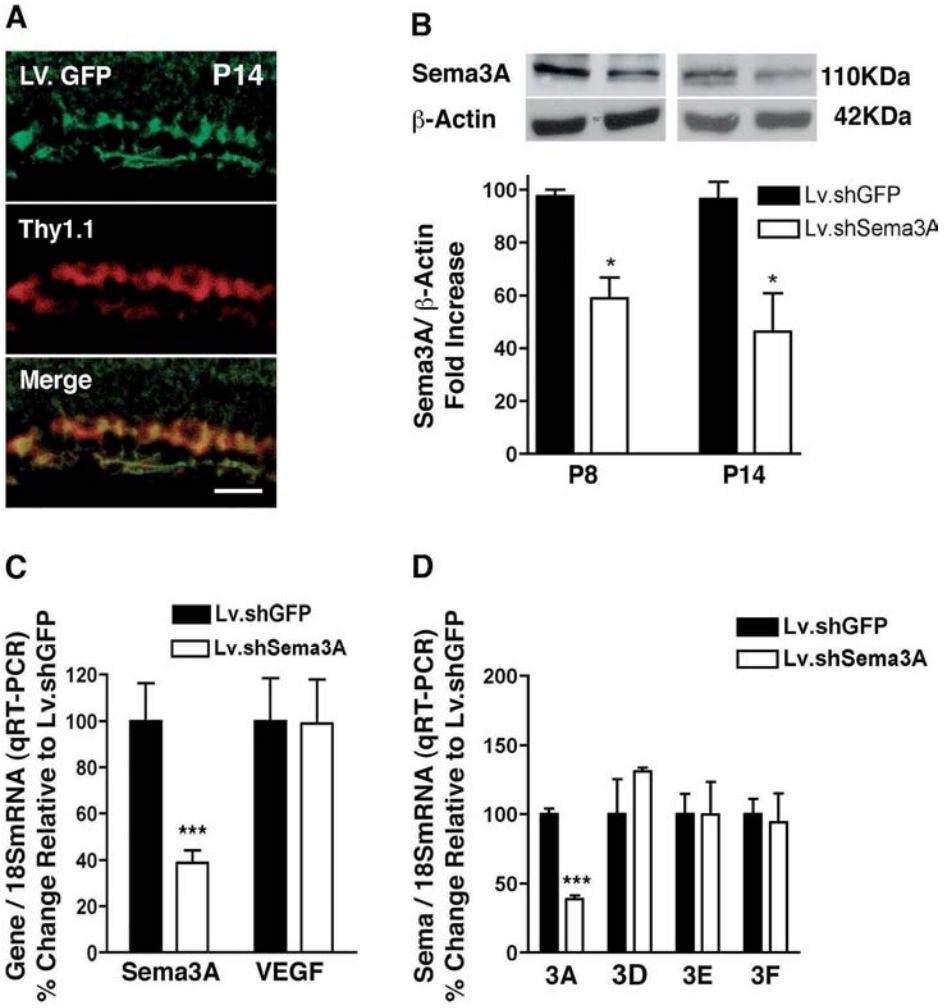
A
LV. GFP
P14
Thy1.1
Merge
B
Sema3A
β-Actin
110KDa
42KDa
Sema3A/ β-Actin
Fold Increase
Lv.shGFP
Lv.shSema3A
P8
P14
C
Gene / 18SmRNA (qRT-PCR)
% Change Relative to Lv.shGFP
Lv.shGFP
Lv.shSema3A
Sema3A
VEGF
D
Sema / 18SmRNA (qRT-PCR)
% Change Relative to Lv.shGFP
Lv.shGFP
Lv.shSema3A
3A
3D
3E
3F

Figure S5

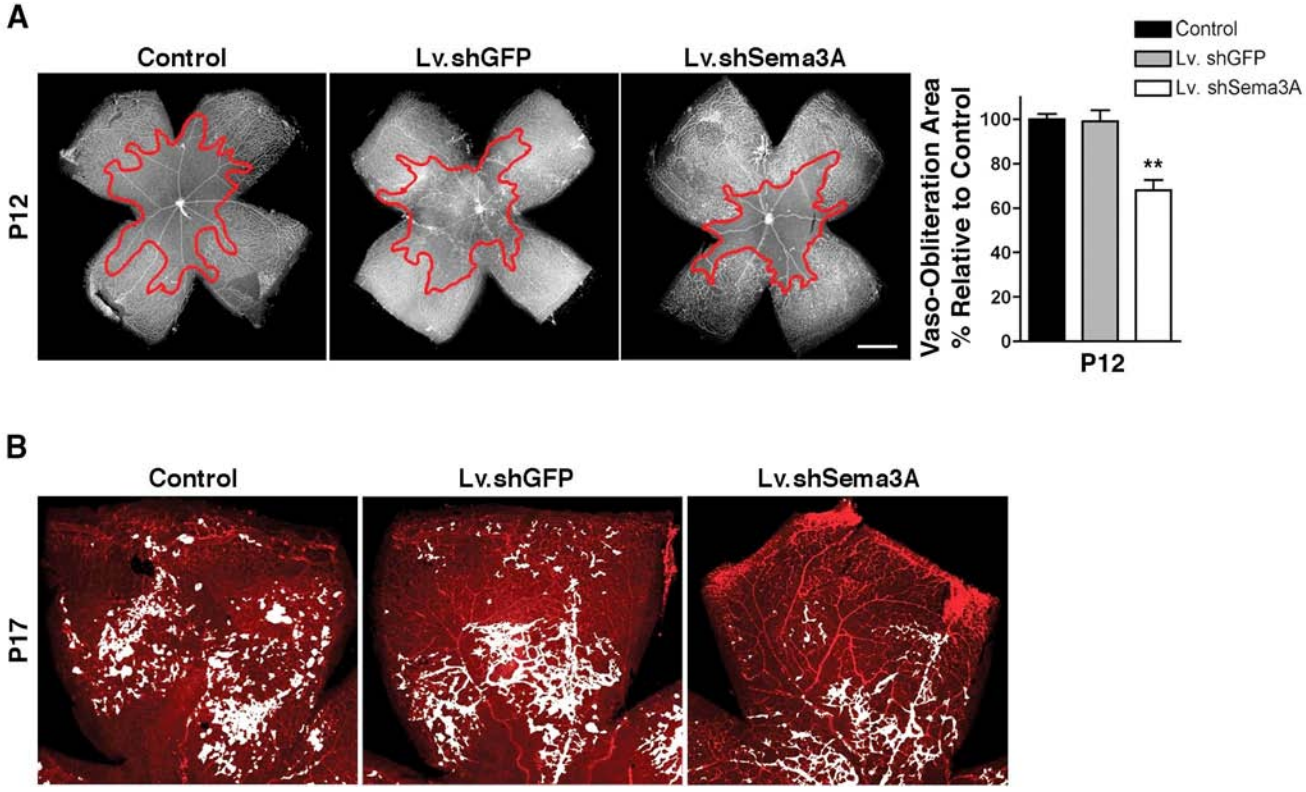
A
Control
Lv.shGFP
Lv.shSema3A
P12
Control
Lv. shGFP
Lv. shSema3A
Vaso-Obliteration Area
% Relative to Control
100
80
60
40
20
0
**
P12
B
Control
Lv.shGFP
Lv.shSema3A
P17

## Figure S6

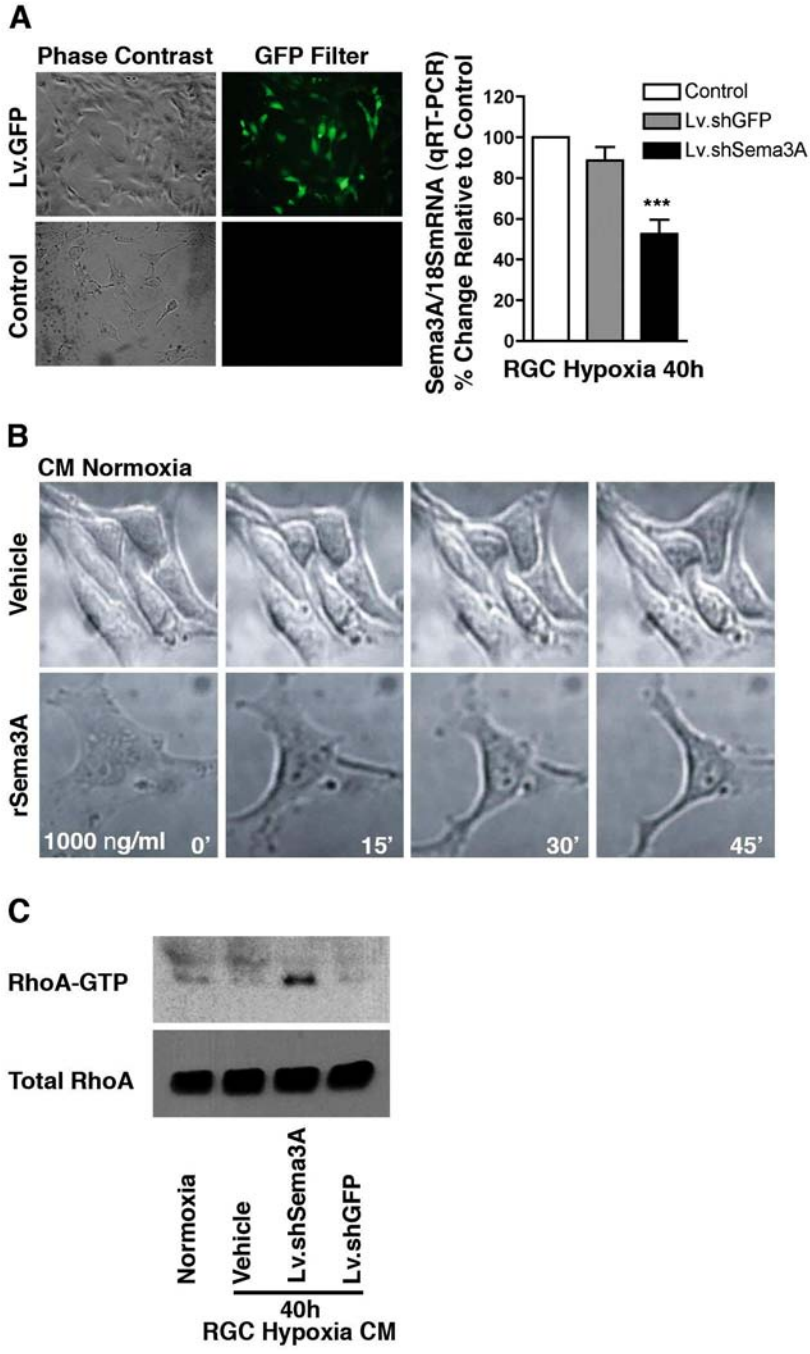
A
Phase Contrast
GFP Filter
Lv.GFP
Control
Sema3A/18SmRNA (qRT-PCR)
% Change Relative to Control
120
100
80
60
40
20
0
Control
Lv.shGFP
Lv.shSema3A
***
RGC Hypoxia 40h
B
CM Normoxia
Vehicle
rSema3A
1000 ng/ml
0'
15'
30'
45'
C
RhoA-GTP
Total RhoA
Normoxia
Vehicle
Lv.shSema3A
Lv.shGFP
40h
RGC Hypoxia CM